ONECENTRAL PRESS

Available online at www.onecentralpress.com

One Central Press

OPEN ACCESS

journal homepage: www.onecentralpress.com/functional-nanostructures

Electrical Profiling and Aptamer Functionalized Nanotextured Surface in a Single Biochip for the Detection of Tumor Cells

*Muhymin Islam,[abc#] Mohammad R. Hasan,[abc#] Adeel Sajid,[acd] Andrew D. Ellington,[e] Young-tae Kim[cfg] and Samir M. Iqbal[*abcfg]*

[a]*Nano-Bio Lab, University of Texas at Arlington, Arlington, TX 76019, USA. [*]E-mail address of corresponding author: smiqbal@uta.edu*
[b]*Department of Electrical Engineering, University of Texas at Arlington, Arlington, TX 76011, USA*
[c]*Nanotechnology Research Center, University of Texas at Arlington, Arlington, TX 76019, USA*
[d]*Department of Interdisciplinary Studies and Department of Biology, University of Texas at Arlington, Arlington, TX 76011, USA*
[e]*Institute for Cell and Molecular Biology, University of Texas at Austin, Austin, TX 78712, USA*
[f]*Department of Bioengineering, University of Texas at Arlington, Arlington, TX 76010, USA*
[g]*Department of Urology, University of Texas Southwestern Medical Center at Dallas, Dallas, TX 75235, USA.* [#] *Equal Contribution*

ABSTRACT

Early detection and accurate enumeration of rare tumor cells in the peripheral blood of cancer patients has enormous diagnostic potential. Highly sensitive approaches are needed for screening and timely diagnosis due to the scarcity of circulating tumor cells (CTCs) at early stages of cancer. Microfluidic devices have emerged as important platforms to detect and quantify tumor cells. This article reports a nanotextured microfluidic device to capture tumor cells with surface grafted anti-EGFR RNA aptamers coupled with translocation behavior based enumeration. Nanotextured polydimethylsiloxane (PDMS) surface was functionalized with aptamers to capture human glioblastoma (hGBM) cells while microchannels on either side of the capture region discriminated tumor cells based on their translocation behavior at single cell level. The translocation profile depended on mechanophysical properties of the cells. First of all, cell capture efficiency and translocation behavior of tumor and blood cells were determined. Eventually, tumor cells were mixed in blood at a concentration of 100 cells/ml and detected using the microfluidic device. The efficiency of the device was above 83% to detect metastatic hGBM cells from blood. The device facilitated multistage detection of tumor cells based on both their mechanophysical and biochemical properties. This lab-on-a-chip approach can be used for cancer screenings at point-of-care.

I. INTRODUCTION

Cancer hallmarks include uncontrolled growth of cells that seize adjacent tissues and often metastasize to remote sites within the body [1]. The detection and enumeration of circulating tumor cells (CTCs) is promising for the diagnosis, prognosis monitoring, assessing metastatic progression, and tracking therapeutic response of cancer patients [2]. The acutely low number of CTCs, ranging from 1-200 in 1 ml of blood, has made it very challenging to detect and enumerate them at the early stages of cancer [3-6]. Many methods have been explored to quantify CTCs including flow cytometry, centrifugation, chromatography, and fluorescence and magnetic-activated cell sorting (FACS and MACS) [1]. These conventional cell sorting techniques are limited due to high cost, low yield, and purity issues and are inconvenient to deploy in point-of-care settings. Consequently, microfluidic platform-based techniques have been developed to recognize and quantify CTCs with various means like mechanophysical interactions [7-11], cell-affinity micro-chromatography [4,12-14], dielectrophoresis [15-18], and magnetophoresis [19-22]. As a recognition element, aptamers have been proven to have higher affinities and specificities towards target cells compared to antibodies [12, 23]. Epidermal growth factor receptor (EGFR) is one of the most common receptors overexpressed on the membranes of tumor cells and it has become an attractive biomarker for cancer diagnosis [24, 25]. It has been reported that primary hGBM cells overexpress EGFR and can be captured using anti-EGFR aptamers [12, 13, 23, 26]. The electrical measurement of ionic current is another approach to discriminate various cell types based on their physical and mechanical properties [3, 5, 27]. This article reports a nanotextured microfluidic device to distinguish hGBM cells from blood cells using aptamer functionalized surface and ionic current measurements. Nanotexturing of the substrate enhanced surface concentration of capturing molecules and improved capture efficiency with minimal nonspecific binding. Electrical profiling of CTCs at the two microchannels offered an additional modality of detection based on their translocation behavior. The method of detection was applied to detect hGBM cells from blood with anti-EGFR aptamer

and can be extended to detect other tumor cells and associated target biomarkers. The nanotextured microfluidic device fabricated in PDMS consisted of an inlet, an outlet, and a cell capture region which was modified with anti-EFGR aptamer, as shown in Fig. 1. The inlet and outlet were on either side of the cell capture zone. Ionic currents were measured across these two channels when cells passed through. These microchannels were small enough to prevent multiple cancer cells travel through together.

It is known that cell capture, growth, adhesion, and orientation are influenced by nanoscale topography of aptamer modified surfaces [12, 28-31]. Nanotextured substrates offer enhanced surface area which amplifies the attachment of aptamers. This increases the probability to capture target cells and reduces the binding of nonspecific cells. Recently, it has been reported by the authors that nanotextured microchannels enhanced the efficiency to distinguish tumor cells from blood when compared to plain microchannels, based just on the translocation behavior [32]. The higher interactions between tumor cells and nanotextured surface selectively changed the translocation time of tumor cells through the two types of microchannels. Micro-reactive ion etching (micro-RIE) was used to create nanotexture on the fabricated microchannel devices. The devices were then functionalized with anti-EGFR aptamer molecules.

The flow velocity was optimized to achieve appreciable capture efficiency for target cells while maintaining reasonable throughput and selectivity. In addition to capturing tumor cells, this device measured ionic current across microchannels to detect them. The translocation mechanism of cells through the microchannels depended on size, shape, orientation, biomechanical properties of the cells, cell-surface interactions, and applied fluid pressure. It has been reported that a number of cancer types depict cells larger in size than blood cells and are highly viscoelastic in nature [5, 33, 34]. The viscoelastic property of tumor cells is different than normal cells due to the transformation of their cytoskeleton as these become malignant [35].

The cells were suspended in phosphate buffered saline (PBS) or blood and translocated through the device under controlled fluidic pressure. While passing the microchannels, every cell triggered a distinctive current pulse due to physical blockage of the channel. First of all, hGBM and white blood cells (WBCs) were suspended separately in PBS to record translocation signatures of respective cell types. The difference in number of detected cells from two microchannels represented the number of cells captured inside the device. The micrographs of the devices were also taken and analyzed to enumerate the number of captured cells in the cell capture zone and compared with current measurement data. Next, the mixture of hGBM and WBCs was used in the experiments. 93% of tumor cells were detected as seen from the analysis of the micrographs of cell capture zone and translocation data of outlet microchannel. Eventually, the hGBM cells were spiked in rat blood at a concentration of 100 cells/ml. More than 83% of tumor cells were detected by the nanotextured microfluidic device. This microdevice has leveraged the virtues of both the cell-aptamer-nanotexture based affinity-chromatography, and mechanophysical properties based current measurement techniques by introducing a combinational approach. This device can be an efficient point-of-care module for the detection of rare CTCs.

II. MATERIALS AND METHODS

Chemicals were purchased from Sigma-Aldrich (St. Louis, MO) unless noted otherwise.

Device Fabrication. The schematic of the microfluidic device is shown in Fig. 1. The inlet and outlet of the device connect to the cell capture zone through two microchannels. The ionic currents were measured at both inlet and outlet. The dimensions of each microchannel were 20 μm x 20 μm x 5 μm (width x height x length). The device pattern was designed in AutoCAD and produced on a glass photomask. The master was fabricated on a silicon wafer, and the device was fabricated using soft-lithography. Specifically, the SU-8 2010 photoresist was spin coated at 1000 rpm for 35 seconds followed by photolithography. Next, PDMS was used to fabricate microfluidic device from the master [32]. Then the device was etched in reactive ion etch series 800 plasma system. The etching was performed using oxygen (O_2) and carbon tetra fluoride (CF_4) for 20 min to create nanotexture. Then devices were washed and functionalized with anti-EGFR aptamer, and covered with UV ozone plasma treated glass slides. The master was characterized using Zeiss LSM 5 Pascal Confocal Microscope and KLA-Tencor Alpha-Step IQ profilometer. Nanotexture of the PDMS substrate has been extensively studied before by the authors [31]. The characterization has included energy-dispersive x-ray spectroscopy, scanning electron microscopy, wettability, etc. To quantitatively evaluate surface topography of the nanotextured PDMS surfaces, a Dimension 5000 atomic force microscope (AFM) was used.

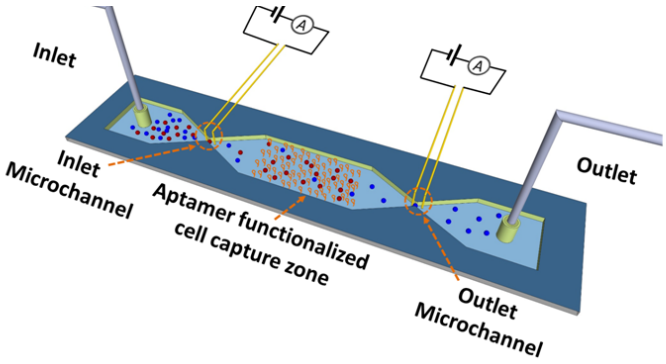

Figure 1 Schematic of the microfluidic device. The device consists of an inlet, an outlet and the cell capture zone which is functionalized with anti-EGFR aptamers.

Measurement Setup. The measurement setup has been reported earlier [3, 5, 6, 32]. The ionic currents were measured across the two microchannels using Ag/AgCl electrodes. A data acquisition card (National Instruments) was used to apply bias voltage and to measure current. A syringe pump (Harvard Apparatus) was used to flow the sample fluid into the device through a tubing adapter.

Aptamer Preparation. Aptamer preparation was done as reported previously [6, 12, 31, 36]. Anti-EGFR RNA aptamer (K_d = 2.4 nM) was used in this study. Aptamer was immobilized on the substrate through duplex formation using amine-modified capture probe. The specificity of the aptamer has been already established in previous works [12, 23].

Attachment of anti-EGFR Aptamer on PDMS Surfaces. The aptamer attachment protocol was adapted from previous work [6, 12, 31, 36]. Briefly, PDMS devices were treated in UV ozone plasma followed by piranha solution dip. These were then immersed in 3% (v/v) of (3-aminopropyl) triethoxysilane (APTES) in ethanol for 30 min at room temperature and cured for 30 min at 120 °C. Next, devices were treated with dimethylformamide (DMF) for 5 hours at 45 °C. Devices were incubated in 30 µmol/l concentration of capture DNA (which had a 5′ amine group) solution overnight in a humid chamber at 37 °C. After washing, samples were immersed in 150 mmol/l DIPEA in DMF and 50 mmol/l 6-amino-1-hexanol for 5 hours and again washed in ethanol, DMF, and DEPC-treated DI water. Then aptamer (1 µmol/l) dissolved in 1X annealing buffer [10 mmol/l Tris (pH 8.0), 1 mmol/l EDTA (pH 8.0), 1 mmol/l NaCl] was placed on each sample. After incubating for 2 hours at 37 °C, samples were washed with 1X annealing buffer and DEPC-treated DI water for 5 minutes. Finally, devices were kept in 1X PBS (pH 7.5) with 5 mmol/l magnesium chloride solution.

Culture of Human Glioblastoma (hGBM) Cells and Collection of Rat Blood. The hGBM cells were cultured using the standard protocol [12, 36]. Lentivirus expressing mCherry fluorescent protein was used to transduce the hGBM cells. The blood samples were collected from the tail of a rat by restraining the animal [32, 38]. Lysis buffer (eBioscience, CA, USA) was used to isolate white blood cells (WBCs) from red blood cells (RBCs) [3, 26, 32]. The cell density was then calculated and 1X PBS was added to achieve desired cell concentration.

Current Measurement and Capture of Cells in Microfluidic Device. The cell suspension was passed through the aptamer functionalized microfluidic devices at different velocities. The current was recorded across two microchannels while cells were passing through. Then 1X PBS was pushed at same flow rate to wash the device and eliminate nonspecifically bound cells. Current was recorded while washing the device to detect loosely bound cells that would dislodge and be detected at the outlet. From the solution, cells were detected by analyzing the data obtained from ionic current measurements. The micrographs of the cell capture zone were also taken with an inverted microscope and analyzed with *ImageJ* to count the captured cells.

First of all, hGBM cells and WBCs were suspended separately in 1X PBS and injected in the device. Next, these two types of cells were mixed at 1:1 ratio and processed through the device. Eventually, hGBM cells were spiked in rat blood at a concentration of 100 cell/ml and pushed through the device. For the mixture of cells, the devices were also imaged with fluorescence microscope to distinguish between cancer and blood cells, as cancer cells expressed mCherry fluorescent protein. In all cases, the experiments were repeated at least twice and average cell capture efficiency was calculated along with standard deviation.

III. RESULTS AND DISCUSSION

Topography of Nanotextured Surface. The average roughness of plain and nanotextured surfaces was approximately 20 nm and 500 nm, respectively. A number of surface roughnesses have been reported in our previous work (from 20 nm to ~630 nm). It has been shown that higher roughness results in better detection efficiency. However, to limit the non-specific binding, an optimum roughness of 500 nm was used in this work [31]. The AFM micrographs of plain and nanotextured surfaces are shown in Fig. 2(a) and 2(b), respectively. The nanotexturing was characterized from the root mean square (RMS) values of the AFM micrographs. AFM tips with radius of ~10 nm (NANOSENSORS™ PPP-NCHR probes) were used for characterization to keep the tip-sample interactions minimal. The sample-tip interaction are known to be negligible for such small tip radii and features as large as 500 nm [37, 43].

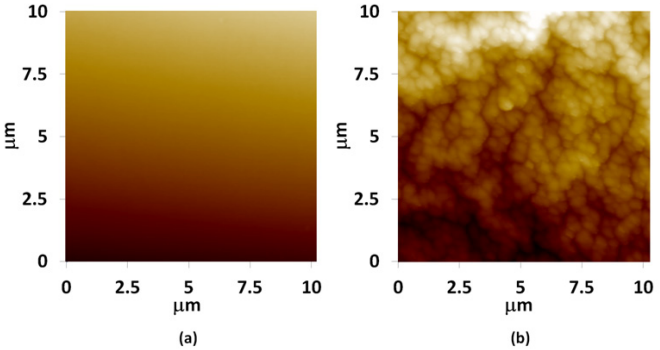

Figure 2 AFM micrographs of (a) plain and (b) nanotextured PDMS surfaces.

Device Assembly. The microfluidic device had two microchannels that was assembled as described in the Materials and Methods section. Dimensions of the microchannels were comparable to average diameter of a tumor cell so that multiple cells could not pass through simultaneously. For the current measurements, frequency of the electrical sampling

was optimized to reduce noise [3, 5, 32]. The current sampling rate was 5 μs (0.20 MHz) and applied bias voltage was 5 volts.

Determination of Cell Capture Efficiency. The hGBM cells have overexpressed EGFR on their membranes and anti-EGFR aptamer has specific affinity towards them [23]. Based on this principle, hGBM cells were captured on the aptamer functionalized nanotextured surfaces. It has been reported before that a flow rate around 2 mm/s can be used to capture tumor cells with high selectivity [26]. Here the flow velocity was varied from 1 to 5 mm/s for observing cell capture performance of the aptamer functionalized nanotextured PDMS. The average diameter of blood cells is smaller compared to many types of tumor cells and WBCs are larger with respect to RBCs [3, 5, 26]. Thus, the probability for hGBM cells to come in contact with aptamer-functionalized surface was higher compared to blood cells inside microchannels. Subsequently, the interactions of hGBM cells with aptamers, and hence their possibility to be captured in aptamer modified nanotextured microfluidic channel, was elevated over blood cells.

First of all, hGBM and WBCs were injected in the device separately to calculate cell capture efficiency. The capture efficiency was defined as the ratio of captured cells and the total number of cells injected in the device. The capture efficiencies of hGBM and WBCs at different flow velocities are shown in Fig. 3(a). As the flow velocity increased from 1 mm/s to 5 mm/s, the capture efficiency for hGBM cells dropped from 79.37±5.97% to 31.79±3.75%. On the other hand, for WBCs capture efficiency decreased from 16.89±4.02% to 3.93±2.59% when the flow velocity went from 1 mm/s to 2 mm/s. Figs. 3(b) and 3(c) show the optical micrographs of captured hGBM and WBCs, respectively at a flow velocity of 1 mm/s.

Another metric for the device performance was the density of probe molecules and overexpression of EGFR biomarker. Cell capture efficiency depended on available number of anti-EGFR aptamers on the surface, the density of EGFR on cell membrane, and the affinity between EGFR and its complimentary aptamer. The number of anti-EGFR aptamer molecules on the surface were enhanced by creating nanotexture on the surface [12]. Higher number of aptamers not only increased the probability to capture many more target tumor cells but also reduced the binding of nonspecific cells. Nanotexture also created minor turbulence in the fluid flow which augmented the possibility of aptamer-cell interactions. The aforementioned phenomenon can significantly amplify the adherence of cells inside the channel. For optimal conditions, aptamer density is usually very high on a surface, roughly estimated to be 20-25 molecules per 100 nm^2, which is almost twenty times higher than the density of EGFR on the cell membrane of hGBM cells [39-41].

The single aptamer-EGFR binding force can be approximated around 8 x 10^{-6} dynes [42].

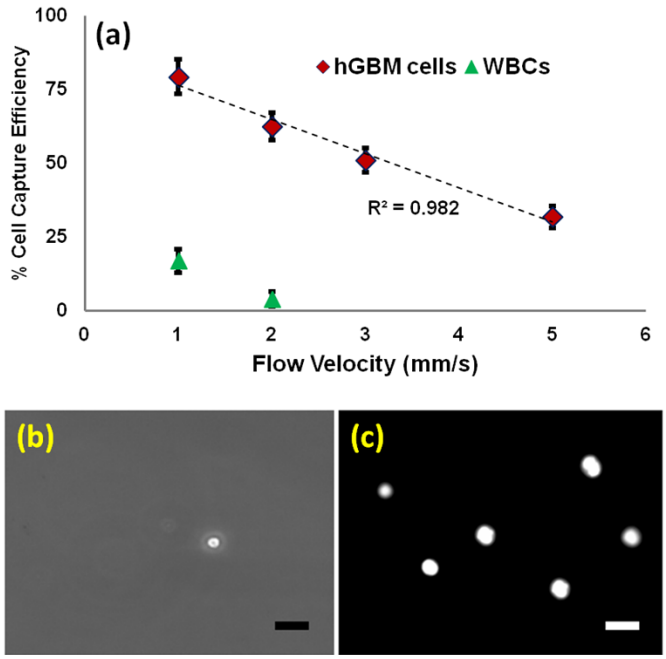

Figure 3 Capture of WBCs and hGBM cells (a). Average cell capture efficiencies on anti-EGFR aptamer functionalized nanotextured PDMS channels at increasing flow velocities for WBCs and hGBM (n = 2); Captured cells (b) WBCs and (c) fluorescent hGBM cells; 50 μm scale bar is for both (b) and (c).

Total binding force between a cell and aptamer grafted surface depends on the EGFR density on cell membrane and total contact area between cell and surface. The size and orientation of cells are also very important for cell-surface binding. The cells with larger diameter are more likely to come in contact with the aptamer grafted surface and become flat to have rigid binding. The higher density of EGFR on cancer cell membranes and larger contact area provided greater binding force. In addition, the flow velocity generated shear stress as well as force on the cell membrane and tried to wash it off. Thus, lower flow rate was favorable for higher capture efficiency.

Electrical Measurement of Cells. Translocation behavior analysis of blood and tumor cells through nanotextured microchannels showed clearly different pulse characteristics (width, amplitude and shape). The current was measured across the two microchannels (inlet and outlet). From the separate hGBM cell and WBC runs at a concentration of 1000 cells/ml, the pulse characteristics of hGBM cells were distinctively different from WBCs. The amplitude and pulse width was higher for most of the tumor cells compared to blood cells. Some hGBM and WBCs had indistinguishable translocation profiles but majority of the tumor cells revealed distinctive behavior. At a flow velocity of 1 mm/s, the average translocation time for hGBM and WBCs were 229±56.62 μs, and 72.79±35.62 μs, respectively. Average peak amplitude for hGBM and WBCs were 19.23±3.67 μA, and 7.68±2.51 μA, respectively. The maximum peak amplitude and translocation time for WBCs

were 15.97 μA and 165 μs, respectively. On the other hand, lowest peak amplitude and translocation time for hGBM cells were 10.41 μA and 125 μs, respectively. Thus, there was an overlapping region in translocation behavior for both types of cells. The calculation showed that 88.68% tumor cells exhibited distinctive behavior in nanotextured microchannels while remaining 11.32% of tumor cells were enveloped in the translocation region of WBCs. The translocation profile of a cell depended on its mechanophysical properties such as size, shape, and elastic modulus, and also on the orientation at a certain flow velocity [3, 5, 32]. The pulse width represented the time a cell took to pass the microchannel. The peak amplitude depended on the cross-sectional area of the channel occupied by cell [6]. The translocation profile of a single cell could vary to some extent based on its orientation. Pulse shape and translocation time also depended on elasticity of a cell. A cell with higher elasticity could pass the microchannel easily resulting in a steady and uniform pulse. Average size of a WBC is generally smaller than an hGBM cell. Again, the tumor cells are highly elastic in nature and can squeeze through small channels quiet easily [33, 34, 38]. The shapes of tumor cells were also different from WBCs. The cumulative effect of all these factors made the translocation profiles of hGBM cells disparate from WBCs as shown in Fig. 4(a).

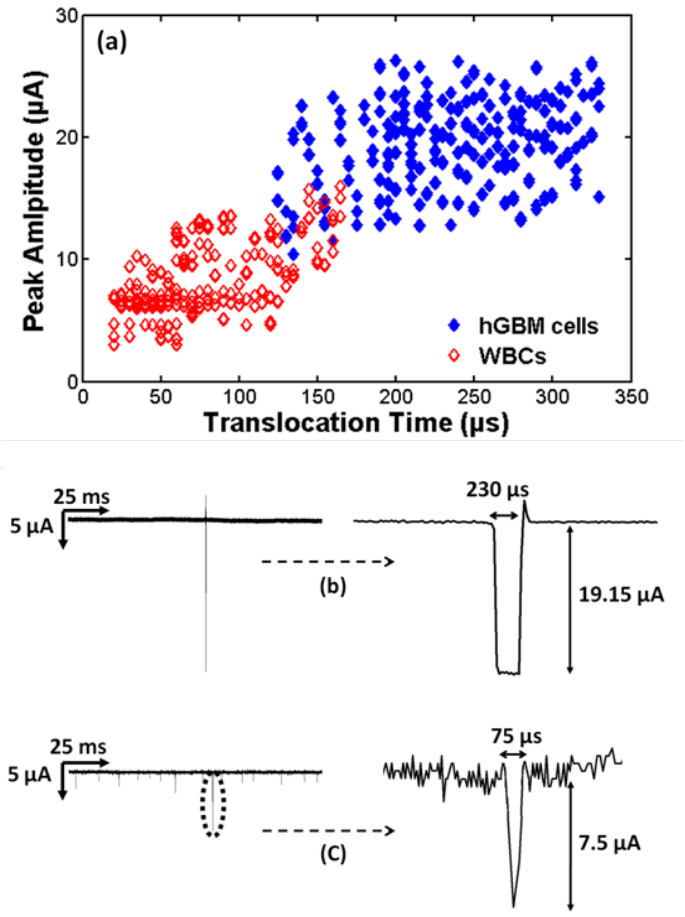

Figure 4 Electrical data and translocation behavior of hGBM cells and WBCs through microchannels. (a) Distribution of the pulses for two types of cells. The average translocation time and peak amplitude of current are larger for hGBM cells (n = 300). Representative pulses of cells translocating through the microchannel: (b) hGBM cells and (c) WBCs.

The flow velocity also influenced the translocation behavior of cells. At higher velocity, the cells moved faster and had less chance to interact with the channel surface. Due to high pressure, cells deformed and resulted in modified pulse characteristics.

Pulse shapes can also be observed closely to differentiate cell types [32]. Due to deformable nature and interactions with the surface, the pulse shapes of cancer cells were different from blood cells (Figs. 4(b) and 4(c)). At a sampling rate of 5 μs and flow velocity of 1 mm/s, on average, a tumor cell and WBC consisted of 46 and 14 data points, respectively. From these data, physical dimension of the whole cell can be depicted. The pulse triggered by a cluster of cells could also be identified from pulse shapes. Generally a pulse from single cell was uniform in contrast to that from a cell cluster. The cluster pulses had several spikes and irregular shapes. Translocation time and peak amplitude for blood and tumor cells were found significantly different from statistical analysis (p-value < 0.01).

Total Detection Efficiency. Tumor cells have distinctive chemical, physical, and biomechanical properties in contrast to blood cells. But the heterogeneity in these properties makes it challenging to detect tumor cells. Thus, this device was designed to take the advantages of all forenamed properties of tumor cells to distinguish them. When only hGBM cells were suspended in PBS solution and passed through the device, the inlet microchannel was used as reference to count the number of cells. The cell capture zone and outlet microchannel were used to capture, and detect these cells. At a flow velocity of 1 mm/s, due to the overexpression of EGFR, this device was able to capture 79.37±5.97% of tumor cells. The remaining un-captured tumor cells were detected as these passed through microchannel at the outlet. In all, 19.16±6.96% of total tumor cells were detected from current measurement data. The detection efficiency was defined as the ratio of detected cells at the outlet microchannel and the total number of cells passed through the device. Hence, 98.53% of tumor cells were detected using the microfluidic devices. Similarly, 96.46±1.84% cells were recovered using the device for WBCs.

As a biosensor, the limit of detection for the device is thus 100 cells/ml where 96 tumor cells can be clearly identified. This is comparable to the number of tumorigenic cells where as few as 100 cells have been shown to develop secondary tumors in immunocompromised host mice [44].

Isolation of hGBM Cells. At early stages of cancer, the number of tumor cells in blood is very low and it is desired to have ultrasensitive devices to detect as many cells as possible. To isolate hGBM cells from WBCs, cells were suspended in 1X PBS at a ratio of 1:1 (2000 cell/ml) and passed through the aptamer functionalized microfluidic devices at 1 mm/s flow

velocity while current was measured across two microchannels. After 30 min, the device was washed with PBS and imaged using a fluorescent microscope. The experiment was repeated twice. The concentration of captured tumor cells and WBCs were measured from micrograph analysis in *ImageJ*. The enrichment of tumor cells inside the device was thus calculated.

For mixture of two types of cells, current pulses had to be assessed minutely to discriminate hGBM cells. The translocation behavior of cell mixtures obtained from inlet and outlet microchannels are shown in Fig. 5(a). These data were compared with the typical translocation behavior obtained from hGBM and WBCs (shown in Fig. 4(a)). Most of the cells showed familiar peaks in both channels. The majority of the cancer cells exhibited higher translocation time and peak amplitude compared to WBCs while some were disguised in the region of WBCs.

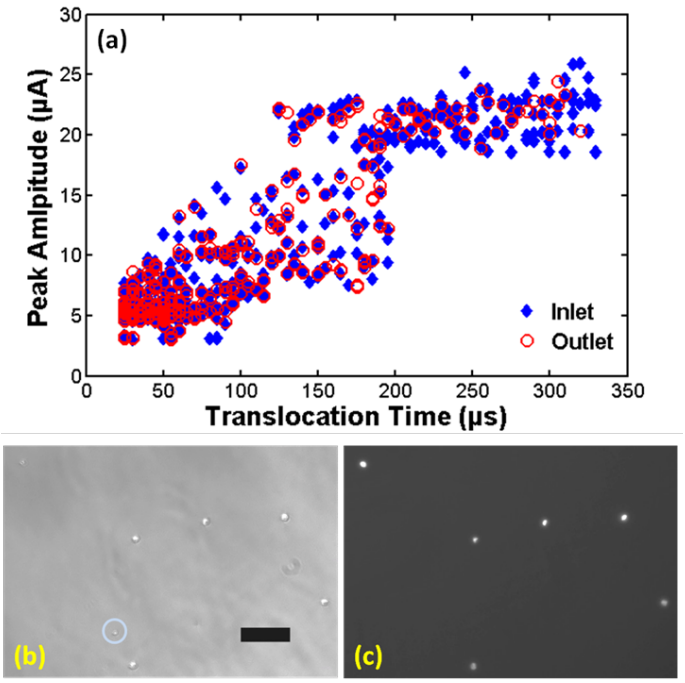

Figure 5 Experimental results for the mixture of hGBM cells and WBCs at a ratio of 1:1. (a) Translocation data for the captured cells on aptamer functionalized nanotextured microdevice (n = 600); (b) Optical micrograph where both types of cells are present (a WBC is marked in blue circle); (c) Fluorescent micrograph of the same place as (b) where only hGBM cells are visible; 100 μm scale bar is for both (b) and (c).

However, translocation data acquired from inlet microchannel of the device was interpreted to detect 82.08±4.91% of the tumor cells. Next, the cell capture efficiency was calculated as 73.36±4.61% from the micrographs as shown in Fig. 5(b) and 5(c). Optical micrograph of Fig. 5(b) shows all the captured cells. Fig. 5(c) is fluorescent micrograph of the same area where only the hGBM cells are visible. Comparison of these images shows a captured WBC which is circled in Fig. 5(b). The data from outlet microchannel identified 20±0.39% of total tumor cells. The cells detected at outlet channel were fewer than the number of cells at inlet channel because majority of the tumor cells (82%) were captured in cell capture zone. The combination of cell capture technique and ionic current measurement offered 93.36% efficiency to discriminate tumor cells from WBCs which is substantially higher compared to either current measurement or aptamer functionalized nanotextured method alone. In addition, cell capture region of the device selectively isolated and enriched the tumor cells over WBCs at a ratio of 4.5:1 (from starting ratio of 1:1).

Detection of Tumor Cells from Blood. Eventually, tumor cells were detected from the mixture of blood sample. First of all, the blood was passed through the device at 1 mm/s flow velocity to record the translocation profile (Fig. 6(a)). The color variation in this plot represents the densities of cells. The maximum peak amplitude, and translocation time for blood cells were recorded as 17.93 μA and 200 μs, respectively.

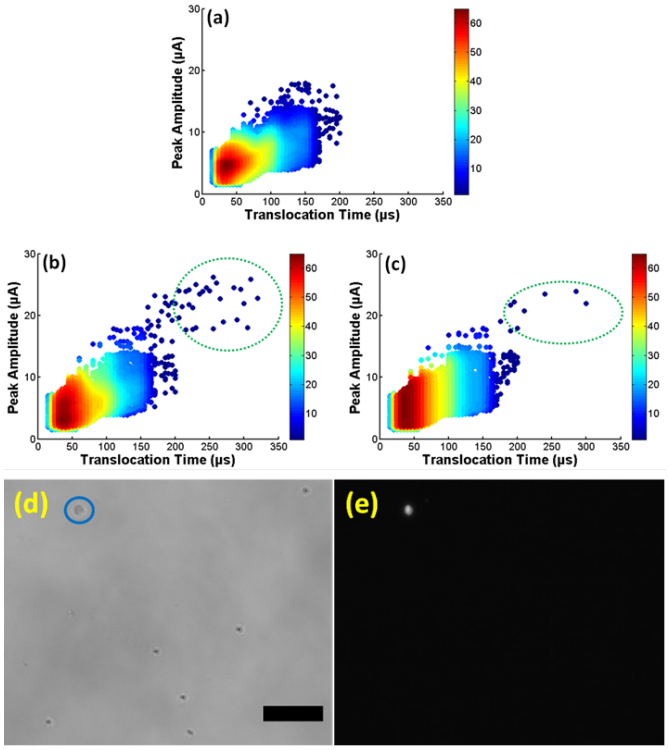

Figure 6 Data for (a) pulses obtained from only blood cells. Blood cells mixed with tumor cells at a concentration of 100 cells/ml (b) at inlet and (c) at outlet. The cancer cells are enclosed in green dotted region. (d) The optical micrograph of captured cells on aptamer functionalized microdevice where both types of cells are visible (an hGBM cell is marked in blue circle); (e) The fluorescent image where only hGBM cell is visible; 100 μm scale bar is for both (d) and (e).

Next, the hGBM cells were spiked in blood at a concentration of 100 cells/ml and this solution was processed through the microfluidic device. After running the experiment for half an hour, images of the device were taken and ionic current data were analyzed from the two microchannels. Fig. 6(b) and 6(c) show the density plots obtained from inlet and outlet microchannels, respectively. The typical translocation profile of hGBM cells were observed before (Fig. 4(a)). By comparing all these figures

tumor cells were detected in both microchannels, as highlighted with green dotted circle in Fig. 6(b) and 6(c). Most of the cells showed familiar peaks in both channels. The majority of the cancer cells exhibited higher translocation times and peak amplitudes that distinguished these from blood cells. However, several cells fell in a region which was very close to blood cells. These small percentages of cells were discriminated by observing pulse shape very closely.

The inlet microchannel was able to detect 70.83% of hGBM cells even at this low concentration of tumor cells. By examining the micrographs, it was calculated that 67.24±8.65% tumor cells were captured in the aptamer functionalized nanotextured region shown in Fig. 6(d) and 6(e). Optical micrograph of Fig. 6(d) shows all the captured cells in the device and Fig. 6(e) is the fluorescent micrograph where only one hGBM cell is visible, marked with blue circle in Fig. 6(d). The overexpression of EGFR, and comparatively larger diameter allowed hGBM cells to interact thoroughly with anti-EGFR aptamer functionalized nanotextured cell capture zone. Consequently, the tumor cells got captured with appreciable efficiency. The outlet microchannel also detected 16.67±3.93% hGBM cells, as recognized from their translocation behavior. The overall efficiency of the device to detect tumor cells was thus 83.91% which was significantly higher compared to the detection efficiency obtained only from translocation behavior of the inlet microchannel or aptamer functionalized cell capture region. The combinatorial approaches should be explored further to meet the challenges of detecting cancer at early stages.

IV. CONCLUSIONS

The primary advantage of this device is that it allowed a multistage and combinatorial scheme to detect tumor cells from blood. Thus, it exploited both the mechanophysical and biochemical properties of the cells to detect them. This nanotextured microfluidic platform detected tumor cells from blood with an efficiency of 83%. The overexpression of EGFR enabled the capture of tumor cells with substantial selectivity and sensitivity. The biophysical properties of cancer cells gave distinctive pulses to detect them from other cell types. The optimized flow rate provided clear selectivity of detection while maintaining reasonable throughput of the device. The application of this device can be extended to detect tumor cells from other bodily fluid samples of patients.

V. ACKNOWLEDGEMENTS

The authors would like to acknowledge useful discussions and help from Azhar Ilyas, Waqas Ali, Nuzhat Mansur and Muhammad Usman Raza. We are also thankful to the staff at Nanotechnology Research Center for their help and training at various stages of the presented work. The work was supported by Cancer Research Foundation of North Texas, Arlington, Texas, USA and National Science Foundation grant ECCS-1407990.

VI. AUTHOR CONTRIBUTIONS

MI and SMI designed the experiments. AS and MRH setup the current measurement system and analyzed the data. ADE developed aptamers. MI and YTK performed experiments. SMI directed the project and supervised this work. All authors have read and approved the final manuscript.

VII. CONFLICT OF INTERESTS

The authors declare no conflict of interests.

VIII. REFERENCES

[1] J. Chen, J. Li, and Y. Sun, "Microfluidic approaches for cancer cell detection, characterization, and separation," *Lab on a Chip,* vol. 12, pp. 1753-1767, 2012.

[2] E. S. Lianidou and A. Markou, "Circulating tumor cells in breast cancer: detection systems, molecular characterization, and future challenges," *Clinical Chemistry,* vol. 57, pp. 1242-1255, 2011.

[3] A. Ilyas, W. Asghar, Y.-t. Kim, and S. M. Iqbal, "Parallel recognition of Cancer Cells using addressable array of solid-state Micropores," *Biosensors and Bioelectronics,* vol. 62, pp. 343-349, 2014.

[4] S. Nagrath, L. V. Sequist, S. Maheswaran, D. W. Bell, D. Irimia, L. Ulkus, M. R. Smith, E. L. Kwak, S. Digumarthy, and A. Muzikansky, "Isolation of rare circulating tumour cells in cancer patients by microchip technology," *Nature,* vol. 450, pp. 1235-1239, 2007.

[5] W. Asghar, Y. Wan, A. Ilyas, R. Bachoo, Y.-t. Kim, and S. M. Iqbal, "Electrical fingerprinting, 3D profiling and detection of tumor cells with solid-state micropores," *Lab on a Chip,* vol. 12, pp. 2345-2352, 2012.

[6] M. M. Bellah, S. M. Iqbal, and Y.-T. Kim, "Differential behavior of EGFR-overexpressing cancer cells through aptamer-functionalized micropores," *Microfluidics and Nanofluidics,* vol. 17, pp. 1-10, 2014.

[7] J. Sun, M. Li, C. Liu, Y. Zhang, D. Liu, W. Liu, G. Hu, and X. Jiang, "Double spiral microchannel for label-free tumor cell separation and enrichment," *Lab on a Chip,* vol. 12, pp. 3952-3960, 2012.

[8] M. Hosokawa, T. Hayata, Y. Fukuda, A. Arakaki, T. Yoshino, T. Tanaka, and T. Matsunaga, "Size-selective microcavity array for rapid and efficient detection of circulating tumor cells," *Analytical Chemistry,* vol. 82, pp. 6629-6635, 2010.

[9] S. Zheng, H. K. Lin, B. Lu, A. Williams, R. Datar, R. J. Cote, and Y. C. Tai, "3D microfilter device

for viable circulating tumor cell (CTC) enrichment from blood," *Biomedical Microdevices,* vol. 13, pp. 203-213, 2011.

[10] H. K. Lin, S. Zheng, A. J. Williams, M. Balic, S. Groshen, H. I. Scher, M. Fleisher, W. Stadler, R. H. Datar, and Y. C. Tai, "Portable filter-based microdevice for detection and characterization of circulating tumor cells," *Clinical Cancer Research,* vol. 16, pp. 5011-5018, 2010.

[11] S. L. Stott, C. H. Hsu, D. I. Tsukrov, M. Yu, D. T. Miyamoto, B. A. Waltman, S. M. Rothenberg, A. M. Shah, M. E. Smas, and G. K. Korir, "Isolation of circulating tumor cells using a microvortex-generating herringbone-chip," *Proceedings of the National Academy of Sciences,* vol. 107, pp. 18392-18397, 2010.

[12] Y. Wan, M. Mahmood, N. Li, P. B. Allen, Y. t. Kim, R. Bachoo, A. D. Ellington, and S. M. Iqbal, "Nanotextured substrates with immobilized aptamers for cancer cell isolation and cytology," *Cancer,* vol. 118, pp. 1145-1154, 2012.

[13] Y. Wan, Y. Liu, P. B. Allen, W. Asghar, M. A. I. Mahmood, J. Tan, H. Duhon, Y.-t. Kim, A. D. Ellington, and S. M. Iqbal, "Capture, isolation and release of cancer cells with aptamer-functionalized glass bead array," *Lab on a Chip,* vol. 12, pp. 4693-4701, 2012.

[14] Y. Xu, J. A. Phillips, J. Yan, Q. Li, Z. H. Fan, and W. Tan, "Aptamer-based microfluidic device for enrichment, sorting, and detection of multiple cancer cells," *Analytical Chemistry,* vol. 81, pp. 7436-7442, 2009.

[15] H. S. Moon, K. Kwon, S. I. Kim, H. Han, J. Sohn, S. Lee, and H. I. Jung, "Continuous separation of breast cancer cells from blood samples using multi-orifice flow fractionation (MOFF) and dielectrophoresis (DEP)," *Lab on a Chip,* vol. 11, pp. 1118-1125, 2008.

[16] F. F. Becker, X. B. Wang, Y. Huang, R. Pethig, J. Vykoukal, and P. R. Gascoyne, "Separation of human breast cancer cells from blood by differential dielectric affinity," *Proceedings of the National Academy of Sciences,* vol. 92, pp. 860-864, 1995.

[17] J. Cheng, E. L. Sheldon, L. Wu, M. J. Heller, and J. P. O'Connell, "Isolation of cultured cervical carcinoma cells mixed with peripheral blood cells on a bioelectronic chip," *Analytical Chemistry,* vol. 70, pp. 2321-2326, 1998.

[18] A. Salmanzadeh, L. Romero, H. Shafiee, R. C. Gallo-Villanueva, M. A. Stremler, S. D. Cramer, and R. V. Davalos, "Isolation of prostate tumor initiating cells (TICs) through their dielectrophoretic signature," *Lab on a Chip,* vol. 12, pp. 182-189, 2012.

[19] M. D. Estes, B. Ouyang, S. Ho, and C. H. Ahn, "Isolation of prostate cancer cell subpopulations of functional interest by use of an on-chip magnetic bead-based cell separator," *Journal of Micromechanics and Microengineering,* vol. 19, pp. 095015-095022, 2009.

[20] A. E. Saliba, L. Saias, E. Psychari, N. Minc, D. Simon, F. C. Bidard, C. Mathiot, J. Y. Pierga, V. Fraisier, and J. Salamero, "Microfluidic sorting and multimodal typing of cancer cells in self-assembled magnetic arrays," *Proceedings of the National Academy of Sciences,* vol. 107, pp. 14524-14529, 2010.

[21] K. Zhang, L. B. Zhao, S. S. Guo, B. X. Shi, T. L. Lam, Y. C. Leung, Y. Chen, X. Z. Zhao, H. L. W. Chan, and Y. Wang, "A microfluidic system with surface modified piezoelectric sensor for trapping and detection of cancer cells," *Biosensors and Bioelectronics,* vol. 26, pp. 935-939, 2010.

[22] C. L. Chen, K. C. Chen, Y. C. Pan, T. P. Lee, L. C. Hsiung, C. M. Lin, C. Y. Chen, C. H. Lin, B. L. Chiang, and A. M. Wo, "Separation and detection of rare cells in a microfluidic disk via negative selection," *Lab on a Chip,* vol. 11, pp. 474-483, 2010.

[23] Y. Wan, Y.-t. Kim, N. Li, S. K. Cho, R. Bachoo, A. D. Ellington, and S. M. Iqbal, "Surface-immobilized aptamers for cancer cell isolation and microscopic cytology," *Cancer Research,* vol. 70, pp. 9371-9380, 2010.

[24] A. Chakravarti, J. S. Loeffler, and N. J. Dyson, "Insulin-like growth factor receptor I mediates resistance to anti-epidermal growth factor receptor therapy in primary human glioblastoma cells through continued activation of phosphoinositide 3-kinase signaling," *Cancer Research,* vol. 62, pp. 200-207, 2002.

[25] A. Franovic, L. Gunaratnam, K. Smith, I. Robert, D. Patten, and S. Lee, "Translational up-regulation of the EGFR by tumor hypoxia provides a nonmutational explanation for its overexpression in human cancer," *Proceedings of the National Academy of Sciences,* vol. 104, pp. 13092-13097, 2007.

[26] Y. Wan, J. Tan, W. Asghar, Y.-t. Kim, Y. Liu, and S. M. Iqbal, "Velocity effect on aptamer-based circulating tumor cell isolation in microfluidic devices," *The Journal of Physical Chemistry B,* vol. 115, pp. 13891-13896, 2011.

[27] J. Chen, Y. Zheng, Q. Tan, E. Shojaei-Baghini, Y. L. Zhang, J. Li, P. Prasad, L. You, X. Y. Wu, and Y. Sun, "Classification of cell types using a microfluidic device for mechanical and electrical measurement on single cells," *Lab on a Chip,* vol. 11, pp. 3174-3181, 2011.

[28] L. Bacakova, E. Filova, M. Parizek, T. Ruml, and V. Svorcik, "Modulation of cell adhesion, proliferation and differentiation on materials designed for body implants," *Biotechnology Aadvances,* vol. 29, pp. 739-767, 2011.

[29] W. Asghar, Y.-T. Kim, A. Ilyas, J. Sankaran, Y. Wan, and S. M. Iqbal, "Synthesis of nano-textured biocompatible scaffolds from chicken eggshells," *Nanotechnology,* vol. 23, p. 475601, 2012.

[30] S. A. Biela, Y. Su, J. P. Spatz, and R. Kemkemer, "Different sensitivity of human endothelial cells, smooth muscle cells and fibroblasts to topography in the nano-micro range," *Acta Biomaterialia,* vol. 5, pp. 2460-2466, 2009.

[31] M. Islam, A. Sajid, M. A. I. Mahmood, M. M. Bellah, P. B. Allen, Y.-T. Kim, and S. M. Iqbal, "Nanotextured polymer substrates show enhanced cancer cell isolation and cell culture," *Nanotechnology,* vol. 26, p. 225101, 2015.

[32] M. Islam, B. Mohammad, H. Mohammad, A. Sajid, Y.-t. Kim, and S. M. Iqbal, "Effects of nanotexture on electrical profiling of single tumor cell and detection of cancer from blood in microfluidic channels," *Scientific Reports,* vol. 5, p. 13031, 2015.

[33] M. Lekka, P. Laidler, D. Gil, J. Lekki, Z. Stachura, and A. Z. Hrynkiewicz, "Elasticity of normal and cancerous human bladder cells studied by scanning force microscopy," *European Biophysics Journal,* vol. 28, pp. 312-316, 1999.

[34] S. E. Cross, Y. S. Jin, J. Rao, and J. K. Gimzewski, "Nanomechanical analysis of cells from cancer patients," *Nature Nanotechnology,* vol. 2, pp. 780-783, 2007.

[35] J. Guck, S. Schinkinger, B. Lincoln, F. Wottawah, S. Ebert, M. Romeyke, D. Lenz, H. M. Erickson, R. Ananthakrishnan, and D. Mitchell, "Optical deformability as an inherent cell marker for testing malignant transformation and metastatic competence," *Biophysical Journal,* vol. 88, pp. 3689-3698, 2005.

[36] M. A. I. Mahmood, Y. Wan, M. Islam, W. Ali, M. Hanif, Y.-t. Kim, and S. M. Iqbal, "Micro+ nanotexturing of substrates to enhance ligand-assisted cancer cell isolation," *Nanotechnology,* vol. 25, p. 475102, 2014.

[37] D. L. Liu, J. Martin, and N. A. Burnham, "Optimal roughness for minimal adhesion," *Applied Physics Letters*, vol. 91, p. 043107, 2007.

[38] M. Islam, W. Asghar, Y.-t. Kim, and S. M. Iqbal, "Cell Elasticity-based Microfluidic Label-free Isolation of Metastatic Tumor Cells," *British Journal of Medicine and Medical Research,* vol. 4, pp. 2119-2128, 2013.

[39] G. Carpenter, "The biochemistry and physiology of the receptor-kinase for epidermal growth factor," *Molecular and Cellular Endocrinology,* vol. 31, pp. 1-19, 1983.

[40] M. Fuentes, C. Mateo, L. García, J. C. Tercero, J. Guisán, and R. Fernández-Lafuente, "Directed covalent immobilization of aminated DNA probes on aminated plates," *Biomacromolecules,* vol. 5, pp. 883-888, 2004.

[41] A. W. Peterson, R. J. Heaton, and R. M. Georgiadis, "The effect of surface probe density on DNA hybridization," *Nucleic Acids Research,* vol. 29, pp. 5163-5168, 2001.

[42] G. I. Bell, "Models for the specific adhesion of cells to cells," *Science,* vol. 200, pp. 618-627, 1978.

[43] T. S. Chow, "Size-dependent adhesion of nanoparticles on rough substrates," *Journal of Physics: Condensed Matter*, vol. 15, p. L83, 2003.

[44] J. Caceres-Cortes, M. Mindeni, B. Patersoni, and M. A. Caligiuri, "A cell initiating human acute myeloid leukaemia after transplantation into SCID mice," *Nature,* vol. 367, p. 17, 1994.

[45] Y. Wan, M. Mahmood, N. Li, P. B. Allen, Y.-t. Kim, R. Bachoo, A. D. Ellington, and S. M. Iqbal, "Nanotextured substrates with immobilized aptamers for cancer cell isolation and cytology," *Cancer,* vol. 118, pp. 1145-1154, 2012.

[46] W. Asghar, Y. Wan, A. Ilyas, R. Bachoo, Y. Kim, and S. M. Iqbal, "Electrical fingerprinting, 3D profiling and detection of tumor cells with solid-state micropores," *Lab on a Chip,* vol. 12, pp. 2345-2352, 2012.